Communication in Physical Sciences, 2023, 10(1): 230-241

The Investigation of the Corrosion Inhibition Efficiency of Aqueous extract of Vernomia Amygdalina for Mild Steel In Various Concentrations of HCl

Richard Alexis Ukpe
Received: 23 May 2023/Accepted 27 November 2023/Published 04 December 2023

Abstract: *The corrosion inhibition potential of Vernomia amygdalona (VA) was investigated using different concentrations of aqueous extract of VA leaves (20 to 140 ppm), which was extracted by the cold process. Gravimetric analysis was carried out to investigate the effect of acid strength (0.4 to 2.0 M HCl), extract concentration and time on the inhibition efficiency of the VA extract. The results obtained showed a higher tendency for the inhibition efficiency to increase with the concentration of the extract but decrease with an increase in the period of contact. Adsorption isotherm fitness based on the Langmuir, Freundlich and Temkin models showed strong correlation coefficients. Physical adsorption. The evaluated values of the free energy of adsorption were below -20 kJ/mol and therefore supported the mechanism of physical adsorption.*

Keywords: *Remediation, environmental consequences, corrosion, mild steel, inhibition, Vernomia amygdalona*

Richard Alexis Ukpe
Federal University Otuoke, Bayelsa State, Nigeria
Email: ukpera@fuotuoke.edu.ng
Orcid id: 0000-0002-1010-4933

1.0 Introduction

Corrosion has persisted as a strong agent against the performance of most metals because of its potential to cause damages through an electrochemical mechanism (Gopalakrishnan, *et al*., 2023). Besides, environmental consequences of corrosion vary from alteration in the quality of the environment through the dissolution of the corroded components to material damages that can create significant imbalances in the ecosystem concerning several cycles (Barghourt *et al*., 2022). Metals corrode when it comes in contact with an aggressive medium such as those media with wide positive and negative variation in pH from the neutral system (Eddy *et al*., 2022a). The manifestation of a suitable corrosion environment has been observed in some industries (including fertilizers, crude oil refining, metallurgical, etc) where metals and the medium interact during processes such as etching, acid washing/cleaning, etc (Eddy *et al*., 2009, 2010).

Due to the aggressive nature of corrosion on the environment, successful abatement procedures have been implemented and even implemented in several workstations and industries respectively (Ferigita *et al*., 2023). Among such remediation programs are anodic/cathodic inhibition, galvanization, coating, etc (Ravi and Peters, 2023). However, the application of substances (called corrosion inhibitors) in minute concentration to the corrosive media has been established as one of the best-known corrosion prevention protocols, termed corrosion inhibition (Betti *et al*., 2023). A wider class of corrosion inhibitors have been enlisted tested and applied at various levels (Wang *et al*., 2023). However, a common mechanism in all corrosion inhibition is the blockage of the active corrosion sites when the inhibitor is adsorbed (Beniken *et al*., 2022).

Therefore, any action that can alter the adsorption process, will certainly alter the inhibition process (ref). Some of the observed requirements for good corrosion inhibitors are the possession of hetero atoms, pi-electron system, conjugated system, aromatic ring, high molecular weight and other properties (Ince *et al*., 2023). An overview of organic compounds have shown significant inhibition efficiencies for various classes of aromatic compounds (Sayed *et al*., 2023). However, due to the toxicity of most compounds, the use of edible plant materials has been widely promoted in recent times (Eddy *et al*., 2022b, 2023). Therefore, the present study is aimed at employing an aqueous extract of *Vernomia amygdalina* (VA) as a corrosion inhibitor for mild steel in a solution of HCl. The employment of this plant extract in corrosion study is not strange because several successful efforts have been documented especially concerning the ethanol extract (Odionngenyi *et al*., 2009), Since the extract composition could be altered by the change in solvent or medium, the use of aqueous extract may have some advantages on the water-soluble components and on the promotion of environmental friendliness.

2.0 Materials and Methods

The mild steel coupons all had dimensions of 2 by 2 by 0.5 m and were carefully polished with different grades of emaryl papers, after degreasing, washing with acetone and allowing them to dry. Weight loss experiments were conducted as widely reported in the literature (ref). Consequently, the corrosion rate (CR) and inhibition efficiency were evaluated using equations 1 and 2 respectively (Abd-elmaksoud *et al*., 2023)

$$CR\ (g/m^{-2}hour^{-1}) = \frac{\Delta w}{At} \qquad (1)$$

$$IE(\%) = \frac{\Delta w}{w_b} \times \frac{100}{1} \qquad (2)$$

Δw is the difference between the weight loss for the mild steel in the blank and inhibited media respectively, t is the period of immersion, A is the surface area of the mild steel and w_b is the weight loss of mild steel in the acidic medium.

3.0 Results and Discussion

3.1 Effect of concentration

Fig. 4.1 shows a plot for the variation of weight loss of aluminium with concentration of HCl. The plot reveals a linear variation of weight loss with concentration of the acid. Since weight loss is a direct measurement of the corrosion rate of a metal, it indicates that the rate of corrosion of aluminium is directly proportional to the concentration of HCl. The linear relationship between weight loss and the concentration of the acid was ascertained by the high degree of linearity (R^2 = 0.989) while the equation for the line was Weight loss = 0.092[HCl], which indicates that the rate of increase of weight loss of aluminium with a concentration of HCl is 0.0242, i.e for every 1 M increase in the concentration of HCl, the weight loss will increase by a multiple of 0.0292.

The corrosion rate of the aluminium coupon in the different test solutions was calculated using the following equation (Al-Amiery *et al*., 2023)

$$CR\ (g.cm^{-2}h^{-1}) = \frac{\Delta W}{At} \qquad (3)$$

where CR is the corrosion rate, ΔW is the weight loss of the metal in g, A is the surface area of the metal coupon (in cm^2) and t is the period of immersion in hours. Consequently, a plot of corrosion rate with time is also a direct measure of the weight loss per cross-sectional area of the metal.

It is also interesting to note that the corrosion rate varied linearly with weight loss (Fig. 2) which is consistent with equation 1. Consequently, the slope of the plot of corrosion rate against the acid concentration (i.e 0.0002 = 1/At), shown in Fig. 2 is an index that depicts the rate at which the surface of the metal coupon (A) changes with time (t) as the corrosion proceeds.

In the presence of the plant extract (VA), the variation of weight loss of aluminium with a

concentration of the extract was also linear over the various acid concentrations range (Fig. 3).

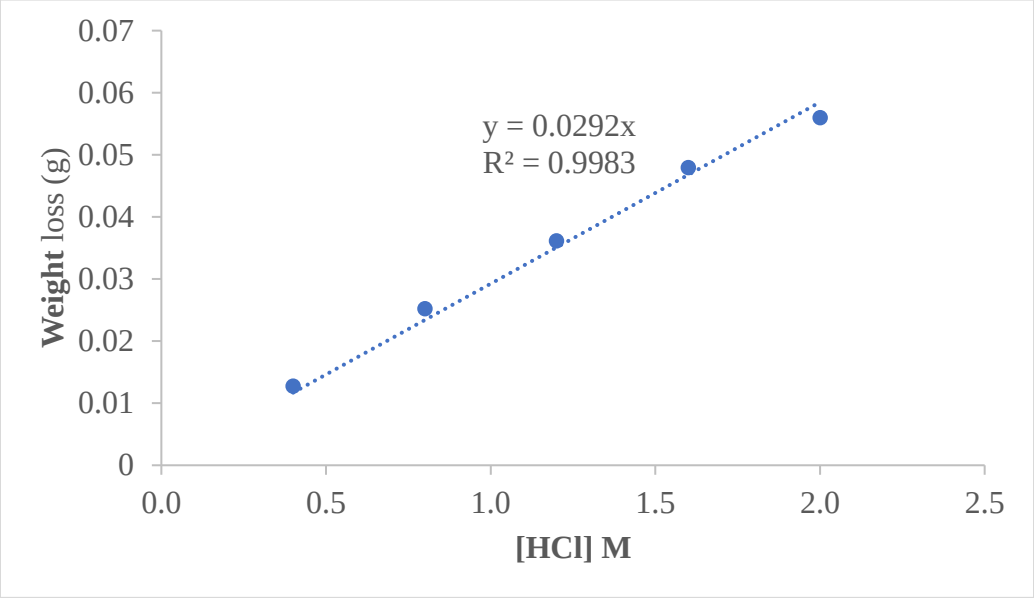

Fig. 1: Variation of weight loss of aluminum with concentration of HCl

Table.1: Corrosion rate of aluminums in various concentrations of HCl

[HCl] M	Corrosion rate (g/cm^2h^1)
0.4	6.63E-05
0.8	0.000131
1.2	0.000188
1.6	0.00025
2.0	0.000292

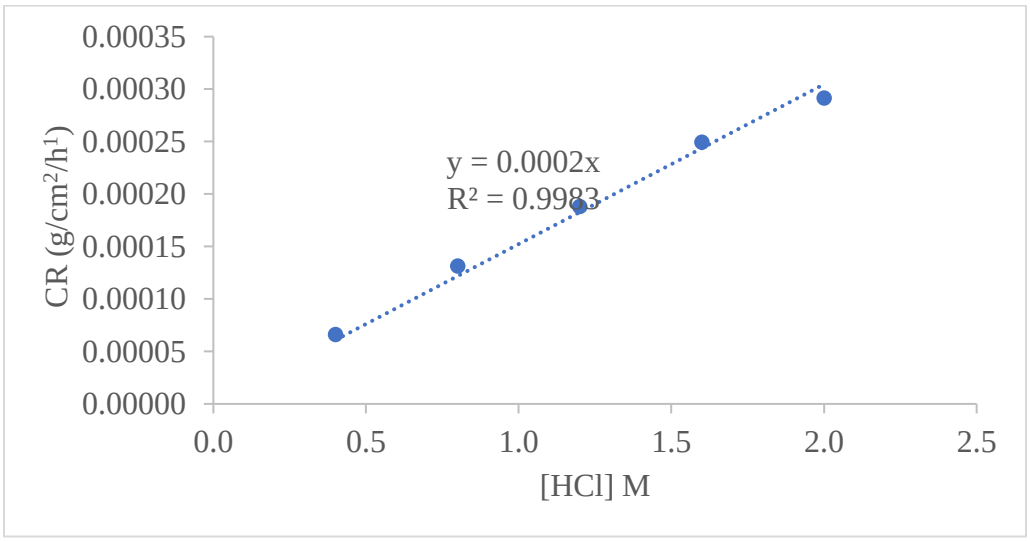

Fig. 2: Variation of corrosion rate of aluminum with concentration of HCl

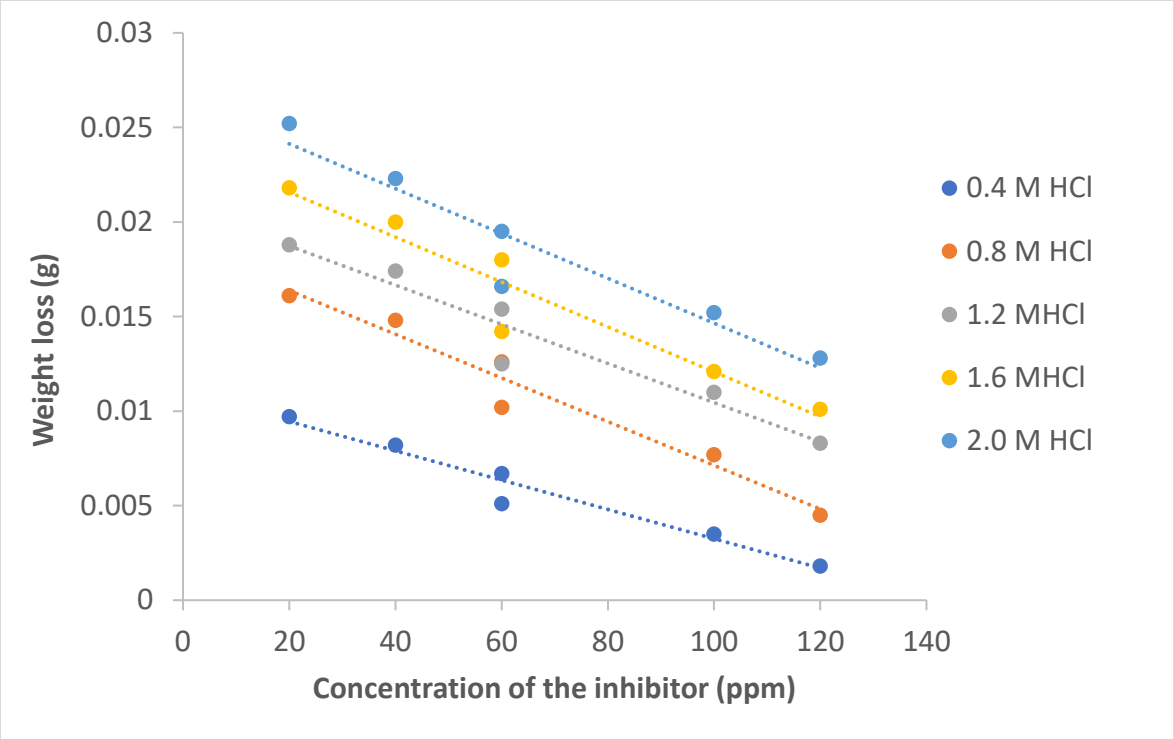

Fig. 3: Variation of weight loss of aluminum with concentration of the inhibitor at various concentration of HCl

Table 3: Corrosion parameters deduced from Fig. 3

[HCl] M	Slope	Intercept	R^2
0.4	0.0001	0.011	0.9561
0.8	0.0001	0.0187	0.9569
1.2	0.0001	0.0208	0.9267
1.6	0.0001	0.0265	0.9086
2.0	0.0001	0.024	0.9147

The significant feature of the plots is the constancy in the slope value (i.e 0.001) for all concentrations of the inhibitor and acids. This indicates that, theoretically, the inhibitor maintained a uniform rate of retardation of the corrosion of aluminium and that the effect of acid concentration on the inhibition rate is minimal. Values deduced from the plots are shown in Table 4.2. R^2 values were all greater than 0.9 indicating excellent fitness of the data to a linear model. A similar pattern was observed for the plots of the variation of the corrosion rate of aluminium with the inhibitor's concentration as revealed by the information presented in Fig. 4 and Table 4. Table 5 shows the corrosion rates of aluminium in various concentrations of the inhibitor in various strengths of the acid. The evaluated corrosion rates increase with an increase in the concentration of the acid but decrease with increasing inhibitor concentration.

4.2 Inhibition efficiency of VA

From the corrosion rates of the metals in the various test systems, the inhibition efficiency of the extract was calculated using the following equation (Gupta *et al*., 2023),

$$IE\% = \left[\frac{CR_b - CR_{inh}}{CR_b}\right] \times \frac{100}{1} \quad (4)$$

where CR_b is the corrosion rate for the blank, CR_{inh} is the corrosion rate for the inhibited system. Calculated values of the corrosion rates for the blank system were presented in Table 2 but the corrosion rates in the presence of various concentrations of the inhibitor are in Table 5. Consequently, calculated values of the inhibition efficiency are recorded in Table 6. The results reveal that the inhibition efficiency of VA extract increases with an increase in the extract concentration irrespective of the strength of the acid. However, between VA concentrations of 20 and 60 ppm, the inhibition efficiency of the extract was observed to increase with the concentration of the acid. This may be due to the tendency of the metal (aluminium) to form a protective layer through passivation at higher concentrations of the acid.

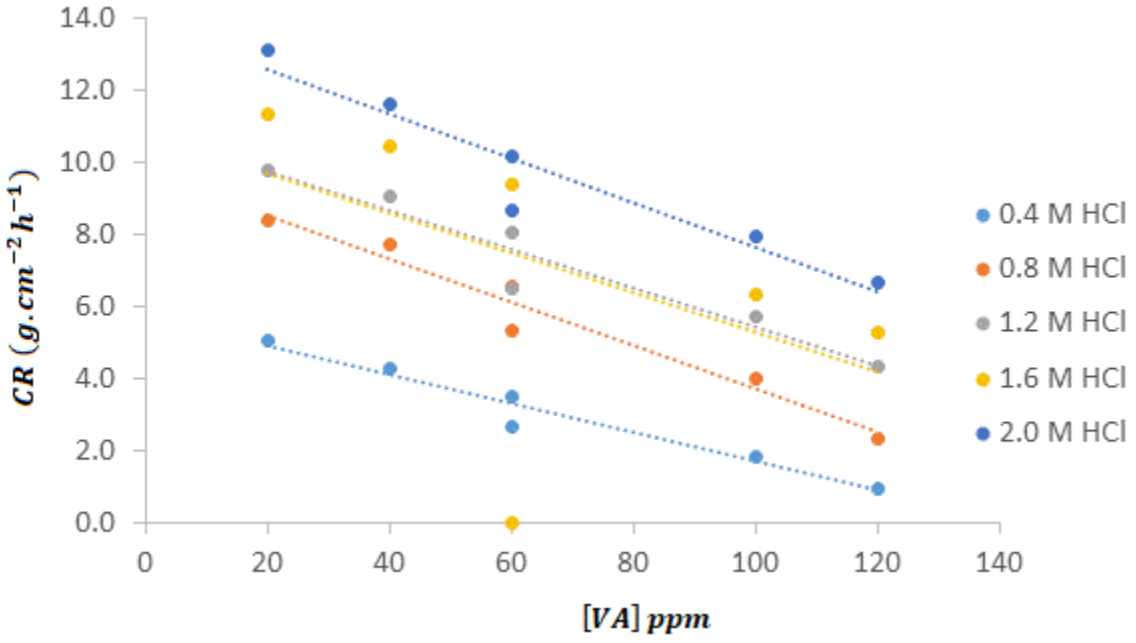

Fig. 4: Variation of the corrosion rate of aluminum with concentration of the inhibitor at various concentration of HCl

Table 4: Corrosion parameters deduced from Fig. 4

[HCl] M	Slope	Intercept	R^2
0.4	0.0404	5.7291	0.9561
0.8	0.0602	9.7336	0.9569
1.2	0.0539	10.835	0.9267
1.6	0.0547	10.767	0.2342
2.0	0.0617	13804	0.9086

Table 5: Corrosion rate of aluminum (x 10^{-5} g/cm^2/h) in various concentrations of HCl containing different concentrations of the inhibitor

[VA] (ppm)	0.4 M HCl	0.8 M HCl	1.2 M HCl	1.6 M HCl	2.0 M HCl
20	5.0521	8.3854	9.7916	11.3542	13.1250
40	4.2708	7.7083	9.0625	10.4167	11.6146

60	3.4895	6.5625	8.0208	9.3750	10.1562
60	2.6562	5.3125	6.5104	7..3958	8.6458
100	1.8229	4.0104	5.7291	6.3021	7.9167
120	9.3750	2.3437	4.3229	5.2604	6.6667

Table 6: Inhibition efficiency of various concentration of the inhibitor in different strength of HCl

[VA] (ppm)	0.4 M HCl	0.8 M HCl	1.2 M HCl	1.6 M HCl	2.0 M HCl
20	23.80	35.50	48.47	54.58	54.74
40	35.58	40.71	52.30	58.33	59.95
60	47.37	49.52	57.79	62.50	64.98
60	59.94	59.13	65.73	70.42	70.19
100	72.51	69.15	69.85	74.79	72.70
120	85.86	81.97	77.25	78.96	77.01

However, at VA concentrations above 100 ppm, the interaction created by the adsorption of the inhibitor onto the surface of the metal overcomes the forces of passivation and the inhibition efficiency started decreasing with an increase in acidic strength. Fig. 5 shows a plot for the variation of inhibition efficiency of various concentrations of VA for aluminium in different acid strengths. The inhibition efficiency varies linearly with concentration indicating that the inhibitor shows a uniform inhibition of corrosion on the surface of the aluminium metal.

4.3 Adsorption study

The degree of surface coverage often shows a defined relationship with concentration for every corrosion inhibition process. In this work, the degree of surface coverage was evaluated using the following equation (Lessa, 2023),

$$\theta = \left[\frac{CR_b - CR_{inh}}{CR_b}\right] \quad (5)$$

Calculated values of the degree of surface coverage are recorded in Table 7. An adsorption isotherm is a model that defines the relationship between the degree of surface coverage and the concentration of the inhibitor at a constant temperature. Such models are based on certain assumptions (ref). Generally, all adsorption isotherms take the form of equation 6 (Alimohammadi *et al*., 2023).

$$f(\theta, x)\exp(-2a\theta) = b_{ads}C \quad (6)$$

where $f(\theta, x)$is the configurational factor which is a function of the physical model and the assumptions that were used in achieving the model, $\theta$is the degree of surface coverage, C is the inhibitor's concentration, x is the size ratio, a is the molecular interaction parameter and b_{ads} is the equilibrium constant of the adsorption. Best-suited adsorption isotherms for the adsorption of VA inhibitor on the surface of aluminium were established through regression fitting and the conformed isotherms included Temkin and Freundlich isotherms.

The Freundlich model is expressed in equation 7 (ref)

$$ln\theta = lnb_{ads} + \frac{1}{n}lnC \quad (7)$$

Freundlcih isotherm for the adsorption of VA on an aluminium surface is shown in Fig. 6. The slope of Freundlich isotherm normally ranges from 0 to unity and is a measure of adsorption intensity or surface heterogeneity. When 1/n is close to zero, a heterogenous surface is defined. 1/n values below unity point toward the chemisorption mechanism but values of the reciprocal of n, above unity, are associated with cooperative adsorption. In this

study, values of 1/n were below close to zero (except in 0.4 M HCl medium (Table .8). Therefore, the adsorption is associated with a heterogeneous surface, indicating the physisorption mechanism for the adsorption of VA on the surface of the aluminium. Also, according to Humpola *et al*. (2013), when the magnitude of the Freundlich constant n is between 1 and 2, moderate adsorption is expected. When n is between 2 and 10, good adsorption is expected but when n is less than 1, poor adsorption is expected.

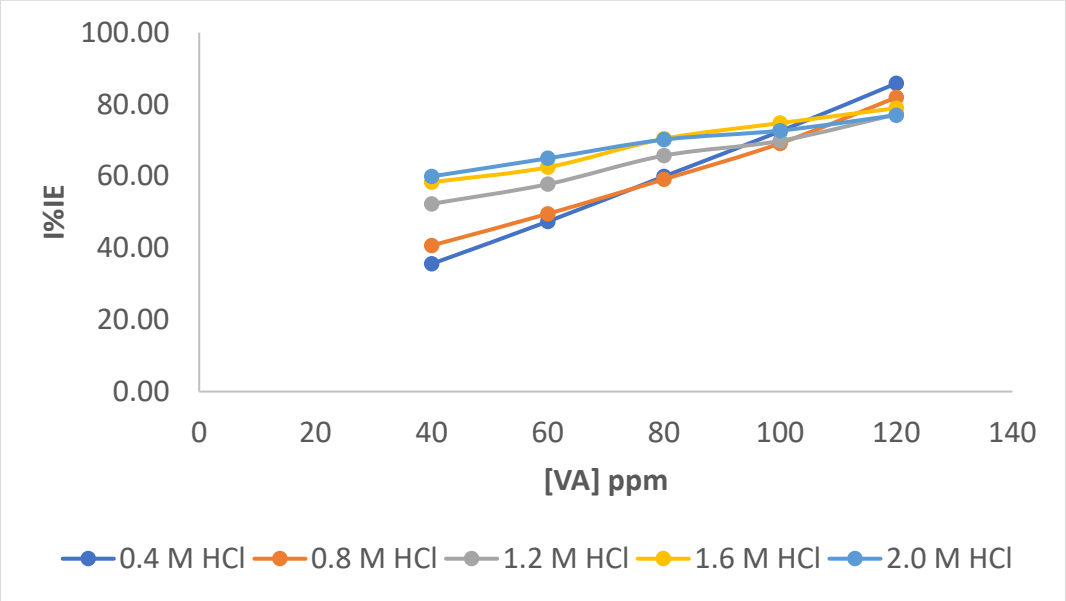

Fig. 5: Variation of inhibition efficiency of VA for aluminium corrosion with concentration in different hydrochloric acid strengths

Table 7: Degrees of surface coverage of the inhibitor on the surface of aluminium

[VA] (ppm)	0.4 M HCl	0.8 M HCl	1.2 M HCl	1.6 M HCl	2.0 M HCl
20	0.2380	0.3550	0.4847	0.5458	0.5474
40	0.3558	0.4071	0.5230	0.5833	0.5995
60	0.4737	0.4952	0.5779	0.6250	0.6498
60	0.5994	0.5913	0.6573	0.7042	0.7019
100	0.7251	0.6915	0.6985	0.7479	0.7270
120	0.8586	0.8197	0.7725	0.7896	0.7701

Therefore since n values for the adsorption of VA on aluminum are between 2 and 10, the adsorption of VA on aluminum surface is good. The standard free energy change is proportional to the logarithm of the equilibrium constant of adsorption (at a given temperature) according to equation 8 (Eddy and Ita, 2011)

$$\Delta G^{*}_{ads} = -RTln(55.5b_{ads}) \quad (8)$$

where 55.5 is the molar concentration of water in the electrolyte. Evaluated values of the free energy are negative, indicating spontaneous adsorption (Table 8). However, they were negatively less than – 40 kJ/mol, which is the threshold value for the chemisorption mechanism. Therefore, the adsorption of VA on the surface of aluminium occurred through the mechanism of physical adsorption. The Temkin model is expressed as equation 9 and simplified to a linear model in equation 9 (ref)

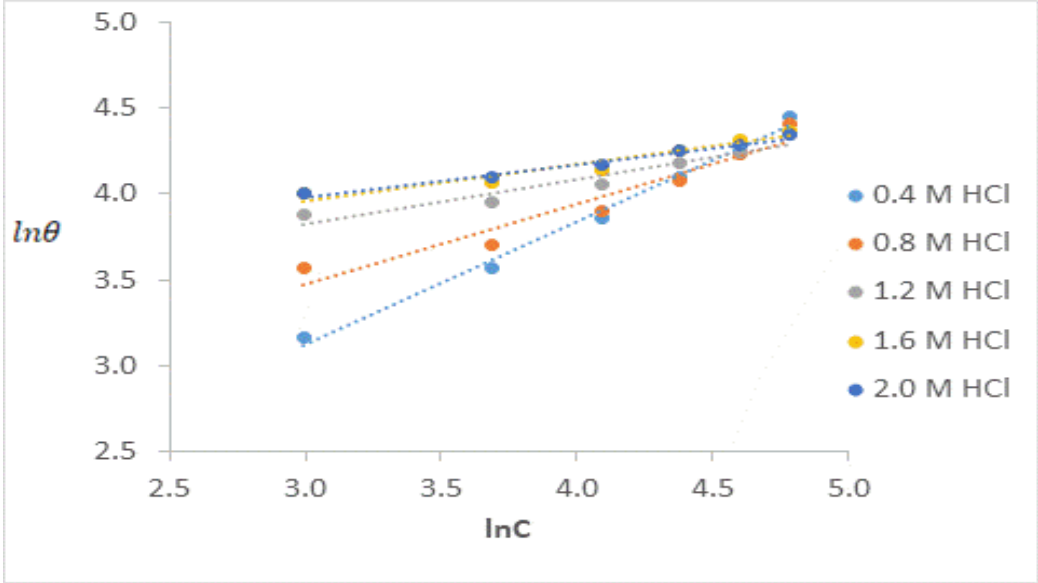

Fig. 6: Freundlich isotherm for the adsorption of VA on the surface of aluminium

Table 8: Freundlich parameters for the adsorption of VA on the surface of aluminium

[HCl] M	1/n	lnb_{ads}	n	ΔG_{ads} $(J.mol^{-1})$	R^2
0.4	0.7152	0.9782	1.40	-2.46	0.9914
0.8	0.4633	2.0874	2.16	-5.25	0.9299
1.2	0.2594	3.0508	3.86	-7.68	0.9279
1.6	0.212	3.3222	4.72	-8.37	0.9288
2	0.1906	3.4118	5.25	-8.59	0.9804

$$\exp(-2a\theta) = b_{ads}C \quad (9)$$

$$\theta = \frac{-lnb_{ads}}{2a} - \frac{lnC}{2a} \quad (10)$$

The suitability of the assumption establishing the Temkin adsorption model to the adsorption of VA on the surface of aluminium was confirmed by the linearity of the plots of θ versus lnC (Fig..7), which is following equation 7. The interaction parameters were not negative and consequently favours the attraction of the adsorbed species (Eddy *et al*., 2018). The mechanism of physical adsorption is also ascertained by the range of values obtained for the free energy of adsorption (Table 9).

The adsorption of VA on aluminium also showed obedience to the Langmuir adsorption model (equation 4.8). This indicated that a plot of ln(C/θ) versus lnC were linear as shown in Fig. 8. Table 10 shows Langmuir adsorption parameters.

$$ln\left(\frac{C}{\theta}\right) = lnC - lnb_{ads} \quad (11)$$

The slopes of the various Langmuir plots were not equal to unity which confirmed deviation from the ideal Langmuir model. Consequently, there exist interaction between the adsorbed species as confirmed by the Temkin isotherm. Excellent linearity was observed from the calculated R^2 (Table 10) and the free energy of adsorption also confirmed the predominance of physisorption mechanism for the adsorption of VA on the surface of aluminum.

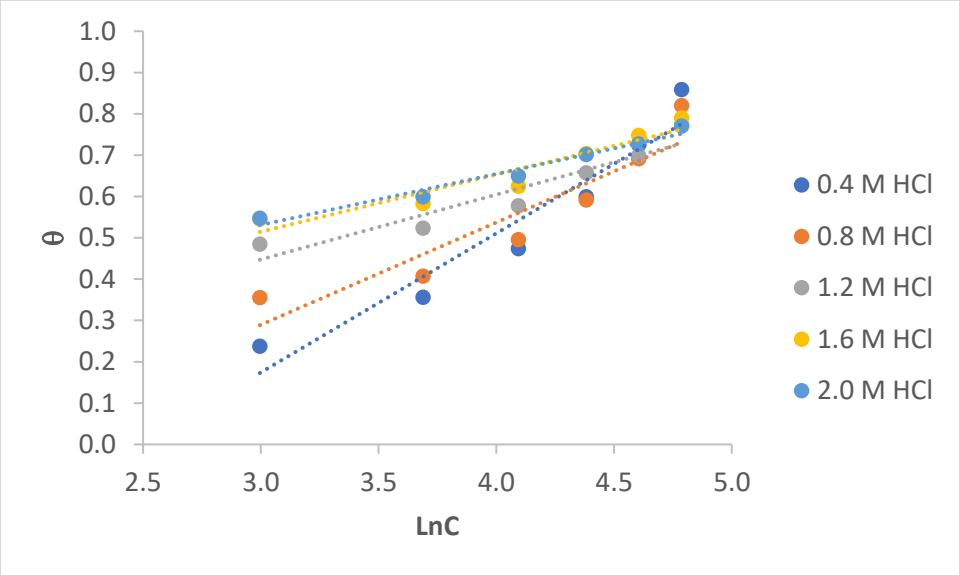

Fig. 7: Temkin isotherm for the adsorption of VA on the surface of aluminum

Table 9: Temkin parameters for the adsorption of VA on the surface of aluminum

[HCl] M	slope	$\ln b_{ads}$	a	$\Delta G_{ads}\ (J.mol^{-1})$	R^2
0.4	-2.48	-3.86	1.49	-8.04	0.9253
0.8	-1.83	-5.51	2.02	-9.00	0.8660
1.2	-0.15	-9.75	3.19	-10.09	0.8966
1.6	0.72	-11.92	3.61	-10.40	0.9074
2	1.30	-13.40	4.05	-10.56	0.9661

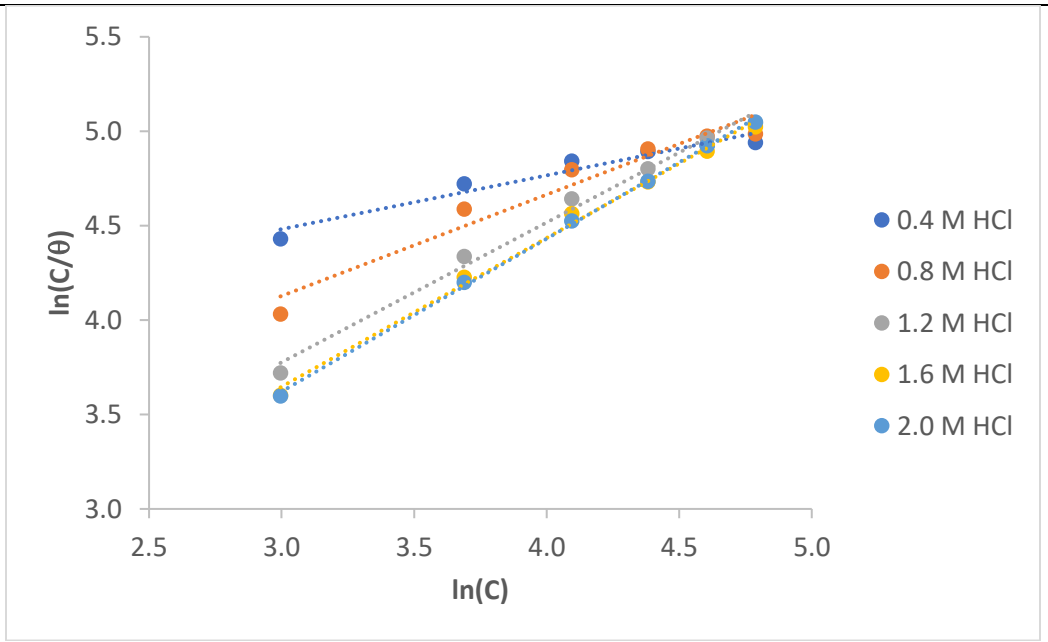

Fi g. 8: Langmuir isotherm for the adsorption of VA on the surface of aluminium

Table 10: Langmuir parameters for the adsorption of VA on the surface of aluminium

[HCl] M	slope	$\ln b_{ads}$	$\Delta G_{ads}\ (J.mol^{-1})$	R^2
0.4	0.2848	3.627	-19.2548	0.9479
0.8	0.5367	2.5178	-16.4605	0.9468
1.2	0.744	1.5544	-14.0336	0.9906
1.6	0.788	1.283	-13.3499	0.9946
2.0	0.8094	1.1934	-13.1242	0.9989

4.0 Conclusion

The present study was conducted to verify the corrosion inhibition potential of aqueous extract of VA and the results show that the inhibition efficiency varied with the concentration of the acid. Adsorption was described by charge transfer from the charged inhibitor to the charged metal surface and showed agreement with the Langmuir, Freundlich and Temkin isotherms.

5.0 References

Abd-elmaksoud, G.A., Abusaif, M.S., Ammar, Y.A. *et al.* (2023). Construction, Characterization, DFT Computational Study, and Evaluation the Performance of Some New *N*-Amino Pyridinone Schiff Base Catalyzed with Ceric(IV) Ammonium Nitrate (CAN) as Corrosion inhibitors in some petroleum applications. *Arab J Sci Eng* , https://doi.org/10.1007/s13369-023-08073-4.

Al-Amiery, A.A., Mohamad, A.B., Kadhum, A.A.H. *et al.* (2023). Experimental and theoretical study on the corrosion inhibition of mild steel by nonanedioic acid derivative in hydrochloric acid solution. *Sci Rep.* 12, 4705, https://doi.org/10.1038/s41598-022-08146-8.

Alimohammadi, M., Ghaderi, M., Ramazani S.A., A. *et al.* (2023). *Falcaria vulgaris* leaves extract as an eco-friendly corrosion inhibitor for mild steel in hydrochloric acid media. *Sci Rep*, 13, 3737 (2023). https://doi.org/10.1038/s41598-023-30571-6.

Barghourt, N. A., El Nemr, A., Abd-El-Nabey, B. A., Fetouh, H. A., Ragab, S. & Eddy, N. O. (2022). Use of orange peel extract as an inhibitor of stainless steel corrosion during acid washing in a multistage flash desalination plant. *Journal of Applied Electrochemistry*, https://doi.org/10.1007/s10800-022-01772-0.

Beniken, M., Salim, R., Ech–chihbi, E., Sfaira, M., Hammouti, B., Touhami, M. B., Mohsin, M. A. & Taleb, M. (2022). Adsorption behavior and corrosion inhibition mechanism of a polyacrylamide on C–steel in 0.5 M H2SO4: Electrochemical assessments and molecular dynamic simulation. *Journal of Molecular Liquids*, 348, https://doi.org/10.1016/j.molliq.2021.118022.

Betti, N., Al-Amiery, A.A., Al-Azzawi, W.K. *et al.* (2023). Corrosion inhibition properties of schiff base derivative against mild steel in HCl environment complemented with DFT investigations. *Sci Rep* 13, 8979, https://doi.org/10.1038/s41598-023-36064-w

Eddy, N. O. & Ita, B. I. (2011). Experimental and theoretical studies on the inhibition potentials of some derivatives of cyclopenta-1,3-diene. *International Journal of Quantum Chemistry* 111(14): 3456-3473. DOI:10.1002/qua

Eddy, N. O., Ameh, P. O. & Essien, N. B. (2018). Experimental and computational Chemistry studies on the inhibition of aluminum and mild steel in 0.1 M HCl by

3-nitrobenzoic acid. *Journal of Taibah University for Science*, 12 (5): 545-556. , https://doi.org/10.1080/16583655.2018.1500514

Eddy, N. O., Ibok, U. J., Garg, R., Garg, R. Falak, A. I., Amin, M., Mustafa, F., Egilmez, M. &. Galal, A. M. (2022a). A brief review on fruit and vegetable extracts as corrosion inhibitors in acidic environments of steel in acidic environment. *Molecules*, 27, 2991. https://doi.org/10.3390/molecules27092991.

Eddy, N. O., Odiongenyi, A. O., Ebenso, E. E.,Garg, R & Garg, R. (2023). Plant Wastes as alternative sources of sustainable and green corrosion inhibitors in different environments. *Corrosion Engineering Science and Technology* , https://doi.org/10.1080/1478422X.2023.2204260.

Eddy, N. O., Odoemelam, S. A. & Odiongenyi, A. O. (2009). Ethanol extract of *Musa species* peels as a green corrosion inhibitor for mild steel: kinetics, adsorption and thermodynamic considerations. *Electronic Journal of Environmental, Agricultural and Food Chemistry*, 8(4):243-255.

Eddy, N. O., Odoemelam, S. A., Ogoko, E. C. & Ita, B. I. (2010). Inhibition of the corrosion of zinc in 0.01 to 0.04 M H_2SO_4 by erythromycin. *Portugaliae Electrochimica. Acta*. 28(1): 15-26

Eddy, N. O., Odoemelam, S. A., Ogoko, E. C., Ukpe, R. A., Garg, R. & Anand, B. (2022b). Experimental and quantum chemical studies of synergistic enhancement of the corrosion inhibition efficiency of ethanol extract of *Carica papaya* peel for aluminum in solution of HCl. *Results in Chemistry*, 100290, https://doi.org/10.1016/j.rechem.2022.100290.

Ferigita, K. S. M., Saracoglu, M., AlFalah, M. G. A., Yilmazer, M. I., Kokbudak, Z., Kaya, S., Kandemirli, F. (2023). Corrosion inhibition of mild steel in acidic media using new oxo-pyrimidine derivatives: Experimental and theoretical insights. *Journal of Molecular Structure*, 1284, https://doi.org/10.1016/j.molstruc.2023.135361.

Gopalakrishnan, V., Balasubramanian, A., Subramanian, L., Muhammed, R. I., Garg, R.,& Eddy, N. O, (2023). Experimental and theoretical analysis on mild steel corrosion inhibition by two novel compounds (FD and ACP) in acidic media. *Portugaliae Electrochimica Acta 41:* 223-246.

Gupta, S.K., Mitra, R.K., Yadav, M. *et al*. (2023). Electrochemical, surface morphological and computational evaluation on carbohydrazide Schiff bases as corrosion inhibitor for mild steel in acidic medium. *Sci Rep* 13, 15108, https://doi.org/10.1038/s41598-023-41975-9.

Ince, A., Koramaz, I., Kaya, E. & Karagoz, B. (2023) An easy route for preparation of carboxylic acid and urea functional block copolymer as corrosion inhibitor, *Journal of Adhesion Science and Technology*, doi: 10.1080/01694243.2023.2240593.

Lessa, R. C. (2023). Synthetic organic molecules as metallic corrosion inhibitors: general aspects and trends. *Organics*, 4, 232-250. https://doi.org/10.3390/org4020019.

Odiongenyi, A. O., Odoemelam, S. A. & Eddy, N. O. (2009). Corrosion inhibition and adsorption properties of ethanol extract of *Vernonia amygdalina* for the corrosion of mild steel in H_2SO_4. *Portugaliae Electrochimica acta* 27(1): 33-45.

Ravi, S. & Peters, S. (2023). Elumalai Varathan, Monisha Ravi, Arockia Selvi J, Molecular interaction and corrosion inhibition of benzophenone and its derivative on mild steel in 1 N HCl: Electrochemical, DFT and MD simulation studies, *Colloids and Surfaces A: Physicochemical and Engineering Aspects*,

661, httpdoi.org/10.1016/j.colsurfa.2023. -130919.

Sayed, A. G., Ashmawy, A. M., Elgammal, W. E. *et al.* (2023). Synthesis, description, and application of novel corrosion inhibitors for CS AISI1095 in 1.0 M HCl based on benzoquinoline derivatives. *Sci Rep* 13, 13761 (2023). https://doi.org/10.1038/s41598-023-39714-1

Wang, X., Liu, S., Yan, J., Zhang, J., Zhang, Q. & Yan, Y. (2023). Recent Progress of Polymeric Corrosion Inhibitor: Structure and Application. *Materials, 16,* 2954. https://doi.org/10.3390/ma16082954.

Compliance with Ethical Standards Declarations

The authors declare that they have no conflict of interest.

Data availability

All data used in this study will be readily available to the public.

Consent for publication

Not Applicable

Availability of data and materials

The publisher has the right to make the data Public.

Competing interests

The authors declared no conflict of interest.

Funding

There is no source of external funding

Authors' contributions

The entire work was carried out by the author